Received: 17 June 2019 | Revised: 3 September 2019 | Accepted: 23 October 2019
DOI: 10.1002/ldr.3486

WILEY

RESEARCH ARTICLE

Conjugation of artificial humic acids with inorganic soil matter to restore land for improved conservation of water and nutrients

Fan Yang[1,2,3] | Shuaishuai Zhang[3] | Qiang Fu[1] | Markus Antonietti[2]

[1]School of Water Conservancy and Civil Engineering, Northeast Agricultural University, Harbin, 150030, PR China

[2]Department of Colloid Chemistry, Max Planck Institute of Colloids and Interfaces, Potsdam, 14476, Germany

[3]Joint laboratory of Northeast Agricultural University and Max Planck Institute of Colloids and Interfaces (NEAU-MPICI), Harbin, 150030, PR China

Correspondence
Markus Antonietti, School of Water Conservancy and Civil Engineering, Northeast Agricultural University, 59 Mucai Street, Xiangfang, Harbin, Heilongjiang 150030, PR China.
Email: antonietti@mpikg.mpg.de

F. Yang, Department of Colloid Chemistry, Max Planck Institute of Colloids and Interfaces, Am Mühlenberg 1, Potsdam 14476, Germany.
Email: yangfan_neau@163.com

Funding information
Natural Science Foundation of Heilongjiang Province of China, Grant/Award Number: QC2018019; University Nursing Program for Young Scholars with Creative Talents in Heilongjiang Province, Grant/Award Number: UNPYSCT-2017018; National Natural Science Fund for Young Scholars, Grant/Award Number: 31600413; Max Planck Society

Abstract

Artificial soil (AS) with a dark–brown appearance and high soil organic matter (SOM) was manufactured under hydrothermal conditions from poor sandy landfill using the 'hydrothermal humification process.' This approach may retrosynthesize the natural clay–humin complex, which is the main contributor for water and ion binding in fertile, natural soils. The structure and morphology of as-created organic–inorganic composites was examined, and it was shown that the as-created artificial SOM (A-SOM) indeed tightly binds to the mineral surfaces, thus creating remediated soil or more general AS. A-SOM does not change the bulk structure of the involved inorganic minerals but activates their surface. Depending on the biomass used as the starting product, the high effectivity of synthetic humification improves the organic carbon and nitrogen content when compared with the employed sandy soil (SS). The composition was adjusted to be comparable with a reference sample of cultivated soil (2.92% in C content and 7.8% in SOM) to enable a fair referencing. We then analyzed the most frequently used soil quality indicators for agricultural land use and found strong water retention and nutrient conservation, which reflects the successful restoration of mineral–humus conjugation. Pure ASs provide superior performance in the analyzed series, whereas simulated soils (mixture of SS and AS) still exhibit satisfactory capacities of water and ion bonding. The values were found to be very similar to cultivated soils sampled from Germany and Harbin, China.

KEYWORDS
artificial soil matter, clay–humin complex, nutrient binding, ion bonding, water binding

1 | INTRODUCTION

Soil can be defined as the medium that provides the foothold and the mineral nutrients for land vegetation, that is, it is the 'dirt' supporting crops (Nikiforoff, 1959). Black soils, classified as dark chernozems and also called mollisols (Yang et al., 2019), are one of the most fertile soil resources for crop production in the world, and there are only three major black earth soil regions in the world. Besides the Northeast China black soil (BS) area, there are two others in the great plains of Ukrainian Plain of Eastern Europe (generally referred to the forest grassland and grassland BS zone of the former Soviet Union) and the Mississippi River Basin of the United States. The area of BS in the great plains of Ukraine and the Mississippi River Basin of the United States is about 1.90 and 1.20 million km^2, respectively. The BS region in Northeast China, which

is covered with a layer of dark-colored soils, that is, BS, chernozem, meadow soil, dark–brown forest soil, brown soil and so on. Black soil in Northeast China is characterized by high organic matter and is a fertile soil in China, with a total area approximately 1.03 million km^2 (Xu, Xu, Chen, Xu, & Zhang, 2010). The three BS regions are distributed in the north temperate zone with four distinct seasons. These three BS areas are most suitable for farming, which store thick humic substances and organic carbon from the incomplete decomposition of biomass partly condensed to BS matter through thousands of years. To feed an increasing world population, severe degradation of BSs took place over the past several decades (Yao et al., 2017). Humic matter is thereby not a lasting gift but can be degraded, depending on conditions even rather fast (Lützow et al., 2006; Schmidt et al., 2011). Unlike the BS in Northeast China, the Ukrainian Plain of Eastern Europe and the Mississippi River Basin of the United States have relatively flat terrain, fewer slopes, and the soil is mainly eroded by wind. On top of consumptive degradation, two 'black storms' have raged in the entire BS region of Ukraine and the United States in the years of 1928 and 1934, along with losing 5–12 cm of soil layer and sweeping away 300 million m^3 of BSs, respectively.

In general, base soil is composed of minerals, organic matter, gases, liquids and organisms, and organic matter and minerals form the main body of the soil. Notably, soil organic matter (SOM) composition resembles typical BS more than other major soil units (Thiele-Bruhn, Leinweber, Eckhardt, Siem, & Blume, 2014), which is a driver for important soil functions like carbon storage and nutrient release (Franko & Merbach, 2017). This can be quantitatively expressed as soil organic carbon contents, and the high (~5–8 wt %) organic carbon content in natural BSs (Yao et al., 2017) make them more fertile (Lal, Negassa, & Lorenz, 2015). Of similar importance, the storage of C in SOM is three to four times higher than the carbon stored in terrestrial vegetation and atmosphere (Lehmann & Kleber, 2015), indicating that it has a crucial role in the global carbon cycle. The climate change thereby could be moderated through storing enormous amounts of C in the soil while decreasing CO_2 concentration in the atmosphere. We consider this as the most feasible tool to control a warming world while using the excess carbon for food production at the same time (Cohen, Pfeiffer, & Francis, 2018; Shepherd, 2016). However, SOM is affected by global change due to the interactions with climate conditions and changes of land management (Franko & Merbach, 2017). Therefore, the stability of SOM in the environment is particularly important for soil quality assessment. The SOC (soil organic carbon) accumulated in mineral soil (SOC_{Min}) exists in soils as labile and stabilized fractions, especially in the topsoil horizon (Grüneberg, Schöning, Hessenmöller, Schulze, & Weisser, 2013), whereas subsoil SOM is more stable (Chabbi, Kögel-Knabner, & Rumpel, 2009). For the stability of SOM in BS, Jin et al. (2016) studied the specific effects of the composition of single soil sources (albic soil [SOMs-A] and BS [SOMs-B]) on the stability of SOM components (^{14}C activity). The results showed that fire-derived aromatic C in SOMs-A is more stable than microbially derived aliphatic C. The higher decomposition of SOMs-B fractions weakened the relationship of their $\Delta^{14}C$ values with the alkyl and aryl C contents.

Natural processes can provide us the leading inspiration to generate thick layers of SOM as in BSs, but they are inefficient and slow as an immediate tool to counteract destructive human interference. Geochemical knowledge is more than sufficient to enable a retrosynthetic approach to mimic humin formation by faster and more efficient chemical processes. As well known, SOM is composed of the humification products of plant residues both above and below ground (primary sources), microbial residues (secondary sources), and various products from chemical decomposition and biochemical activity (Haberhauer, Rafferty, Strebl, & Gerzabek, 1998). Our previous work demonstrated the feasibility of carbon sequestration simulating natural coalification by hydrothermal chemical approaches (Hu et al., 2010; Titirici, Thomas, & Antonietti, 2007), and concurrent work has realized successful fabrication of humic substances from crude biomass (F. Yang, Zhang, Cheng, & Antonietti, 2019). Under the applied mild condition, the hardly convertible lignin in biomass reacts together with organic acids and dehydrated sugars, and most analytical parameters of the products are practically indistinguishable from organic matter isolated from real soil. This follows elder knowledge where scientists described interrelation of natural organic acids and lignins in the natural soil formation process (Marshall & Page, 1927).

In the present paper, we describe an attempt to transform poor sandy soil (SS) from a landfill operation into 'new BS' through a one-step conversion process, in which the physical and chemical properties of color change and mineral composition and structure are similar to real BS. The soil carbon content in the new BS is increased, which will facilitate the activation and integration of soil minerals. Worth noting, soil fertility aligns to crop yields represents agricultural productivity (Bünemann et al., 2018; Patzel, Sticher, & Karlen, 2000), which is described as 'the ability of the soil to supply essential plant nutrients and soil water in adequate amounts and proportions for plant growth and reproduction, in the absence of toxic substances which may inhibit plant growth' (www.fao.org). The ability to bind water and nutrients thereby are two important indicators for soil quality. These quantities are determined for the model artificial soils (AS) and compared with the corresponding values or cultivated Germany soil and Chinese BS.

This contribution is part of a series where we aim to prepare humic substances and SOM only using an easy hydrothermal process (hydrothermal humification [HTH]) on the base of crude biomass leftovers or agricultural 'waste' for large-scale land remediation. It is clear that we can only present a first set or scientific fundamentals, and many other aspects require the involvement of the agricultural stakeholders and end users to a much larger degree than practiced to date.

2 | MATERIALS AND METHODS

Unless otherwise noted, all of the commercial reagents were used as received. Glucose (purity > 98.0%), potassium chloride (KCl; purity > 98.0%), ammonium chloride (NH_4Cl; purity > 98.0%), sodium dihydrogen phosphate (NaH_2PO_4; purity > 98.0%), and potassium hydroxide (KOH; purity > 98.0%) were purchased from Sigma-Aldrich.

Wood powders, eucalyptus leaves, SSs, and cultivated soils were collected in the campus of Max Planck Institute of Colloids and Interfaces, Potsdam, Germany. Black soils for comparison were sampled in the campus of Northeast Agricultural University, Harbin, China. Before experiments, the rude biomass should be cut into a suitable size. Typically, 1.20-g rude biomass powders, 5-g SS, and various KOH qualities (ensuring the molar rations between degradable cellulose and alkali close to 1) were put into the bottom of the glass tube in 50-ml autoclave in the oven to heat to 200°C and then keep for 24 hr to ensure the sufficient coalification. After the temperature naturally cooled down to room temperature, the AS with brown color can be obtained after subsequent drying procedure. All solutions were prepared with ultrapure water (Millipore, 18 MΩcm) for both material preparation and adsorption experiments. Typically, SOM examination of SS, AS, and cultivated soil is also carried out following the procedures: first, the open space was placed in a muffle furnace, burned at 95°C for 30 min, taken out and cooled in a desiccator for 20 min, and the mass was weighed; then, it was burned at the same temperature for 30 min, taken out, cooled, and weighed. Repeated the above steps until the mass difference between the two times is less than 0.5 mg. Weigh about 0.50 g of dry sample in a known quality crucible, put it in an oven at 105°C for 12 h, then take it out, put it into the desiccator, cooled it, weighted it, and recorded the quality; next, transfer the crucible to a muffle furnace and heat up to 550°C, burn for 5 hr, cool in a desiccator, weigh, and record the mass and calculate. Basic mineralogical properties of soil samples were listed in Table S1. Additionally, a glucose model as well as two different models of crude biomass were humified in the presence of a controlled amount of base, and the resulting humic–mineral complexes were characterized by scanning electron microscopy (SEM), elemental analysis (EA), energy dispersive X-ray (EDX), and Fourier-transform infrared spectroscopy (FTIR) analyses.

FIGURE 1 A photograph of the actual location for sampling poor sandy soil at the MPI Golm campus, Germany, as left after building operations. The insert depicts the appearance of sandy soil and this soil after conjugation with artificial humic acids [Colour figure can be viewed at wileyonlinelibrary.com]

3 | RESULTS AND DISCUSSIONS

Our starting point is a rather low-quality SS sampled at the location of our institute, as it is typical for land refilling after building operations and 10 years of spontaneous recultivation. Figure 1 depicts the sampling location just below the thin weak new cultivation layer (0–20 cm). One can see the typical yellow to yellow–gray fine powder sand with uniform texture, rich in calcium or nodules with prominent vertical joints. These characteristics in structure and components cause that water seepage is easy, as it is to be eroded by water to form gullies, and also to cause subsidence and collapse. Left-alone recultivation thus provided only thin humus horizons, poor soil carbon content, and a very low ability of water and nutrient conservation (Cui

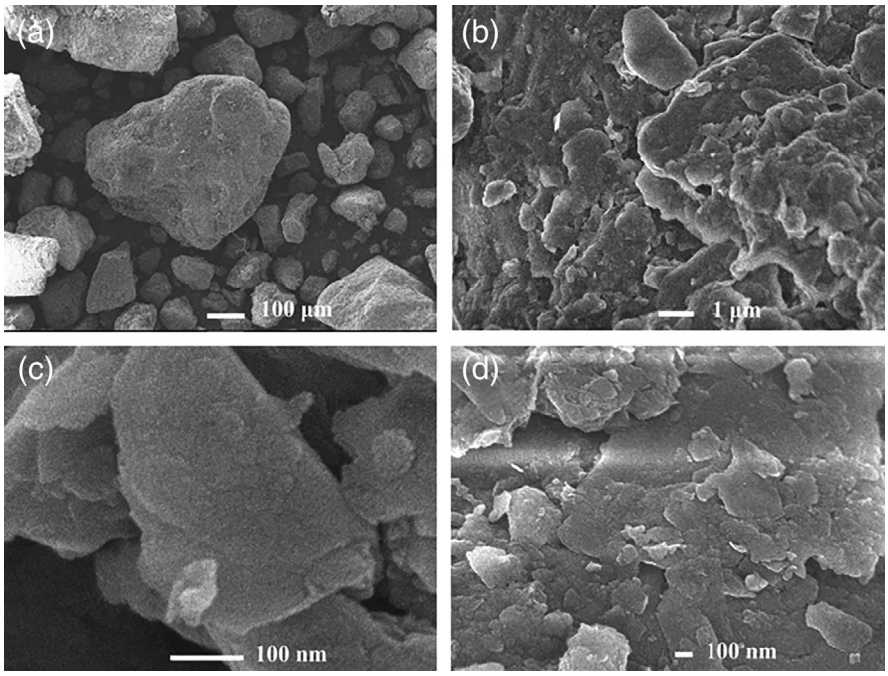

FIGURE 2 Low- and high-magnification scanning electron microscopy images of the sandy soil sample from a refilled construction site

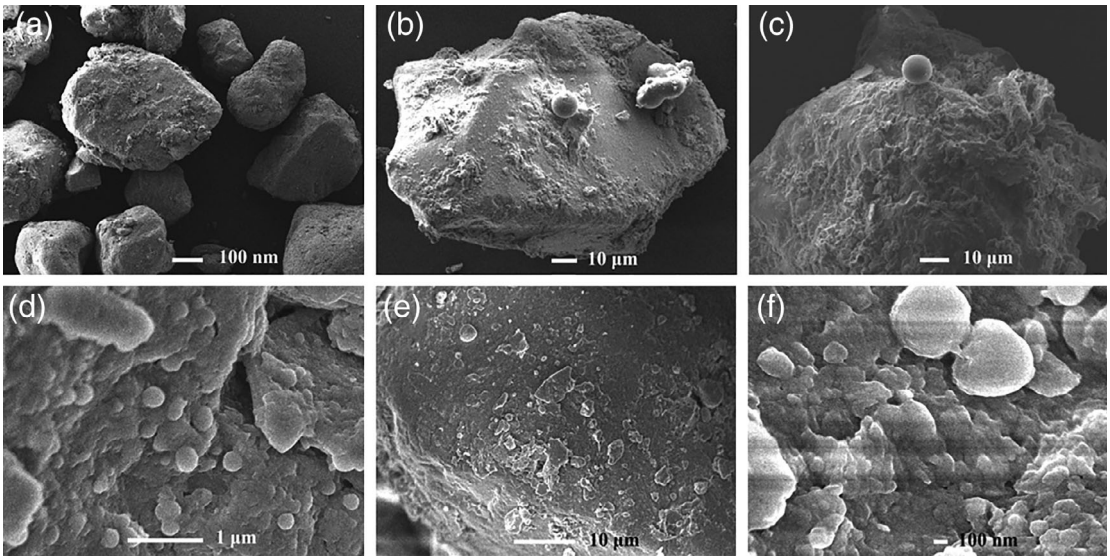

FIGURE 3 Low- and high-scanning electron microscopy images of glucose-based artificial soil

et al., 2018). The AS made from those structures in the insert already exhibits a dark brown, near to black color, similar to cultivated soil from appearance (Figures S1 and S2) and also the SOM content has changed positively.

In HTH technology, crude plant biomass is added to the soil minerals, and the mixture is 'cooked' with a certain amount of KOH in an autoclave under anaerobic conditions. Applying temperatures of the order of 200°C and autogenous pressure for a few hours greatly accelerate the humification process. The amount of biomass is directly related to the SOM content and contrary to composting, most of the carbon indeed is kept in the soil. Doing the humification in the presence of the minerals enables mineral activation with abundant —OH functionalities by the starting base, endowing them a more hydrophilic character, and the organic acids formed later in the process promote a tight conjugation of organic matter with the surface of the minerals, a structure mimicking the mineral–humus complex (Varadachari, Mondal, Dulal C., & Ghosh, 1994). This also avoids separation of the organic matter by liquid water towards floating macroscopic organic patches, as it generally found for mixed-in compost (Liu et al., 2018).

For a microscopic view on this process, low- and high-magnification SEM images are taken and displayed in Figures 2–5. The particles of SS have a relatively smooth surface, with sometimes sheet-like fracture splits (Figure 2). For the model glucose-based AS (G-AS) sample (Figure 3), the mineral surfaces are coated after the humification progress, and thin layers of sugar-derived biochar can be recognized (Figure S3). Besides, a large amount of surface bound floccules as well as various sized sphere-like particles are found in Figure 3 too, indicating either incomplete binding or simply a too high excess of carbon source: The increase of soil carbon and organic matters is mainly due to the introduction of artificial fulvic acids, the product obtained from the model glucose as described for the pure product in our previous paper.

Figures 4 and 5 depict the microstructure of AS samples for humic matter from more complex biomass sources. Here, we used the fruit stands of tulip tree (leaf-based artificial soil, L-AS) and sawdust of beech core wood (wood-based artificial soil, W-AS) as models for lignocellulosic waste biomass. Some spherical hydrochar particles with a wide range of sizes are also found in those real biomass samples (as presented in Figures S4 and S5), along with fibers and other particles with biological texture, structural reminders of the natural biomass precursors due to the presence of lignin, that cannot be degraded under such mild hydrothermal reaction conditions. However, a majority of humic substances is found to be tightly bound to the soil minerals, constituting the synthetic SOM (A-SOM). This indeed is very similar to the appearance of organic matter in real soil. Literature reports that natural organic acids and lignin derivatives occur in close relation and that the natural humification process obviously results in coexistence of weakly modified lignins with condensed organic acids (Marshall & Page, 1927).

The natural huminogenesis involves biological, physical, and chemical processes to convert dead plant materials into organic soil matter that are able to form intimate associations with soil minerals (Lehmann & Kleber, 2015). However, due to the predominant metabolization of the biomass as such, the efficiency of this cascade is only low. The whole hydrothermal reaction is purely chemical and very efficient with respect to the carbon yield, as practically all carbon of the waste biomass is contained in the final material. Worth noting, in spite of the rather high amounts of added base, we have examined the pH in SS and BS before and after the hydrothermal reaction and found 7.22 versus 7.10 and 6.85 versus 6.76, respectively, indicating that the transformation of biomass into organic acids and biochar in the presence of the added base is essentially pH buffered. It progresses until neutrality is reached, and the soil after manufacturing can be used as such. We assume that the larger fulvic and humic acids are strongly bonded to the soil minerals to form intimate associations

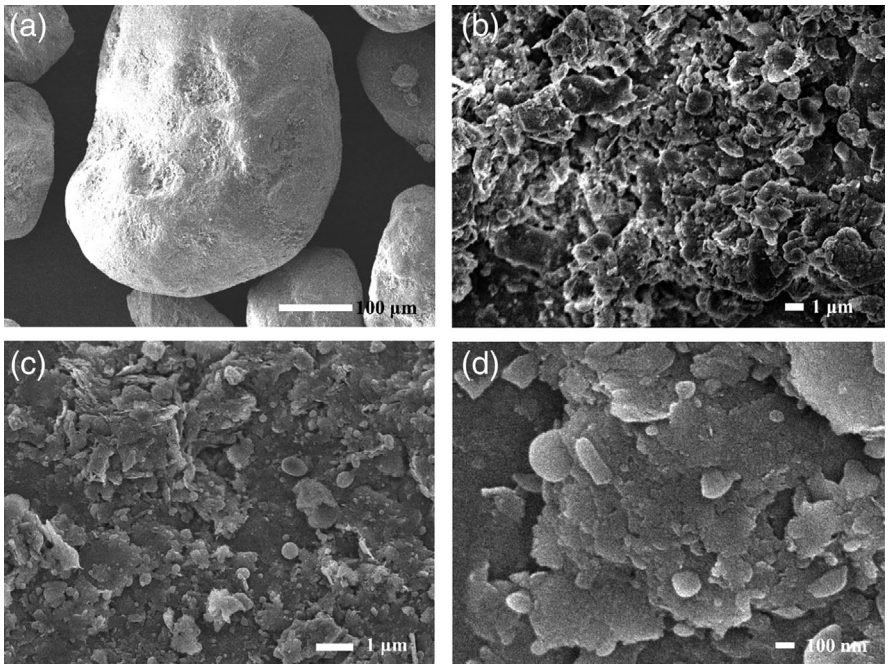

FIGURE 4 Low- and high-scanning electron microscopy images of wood-based artificial soil

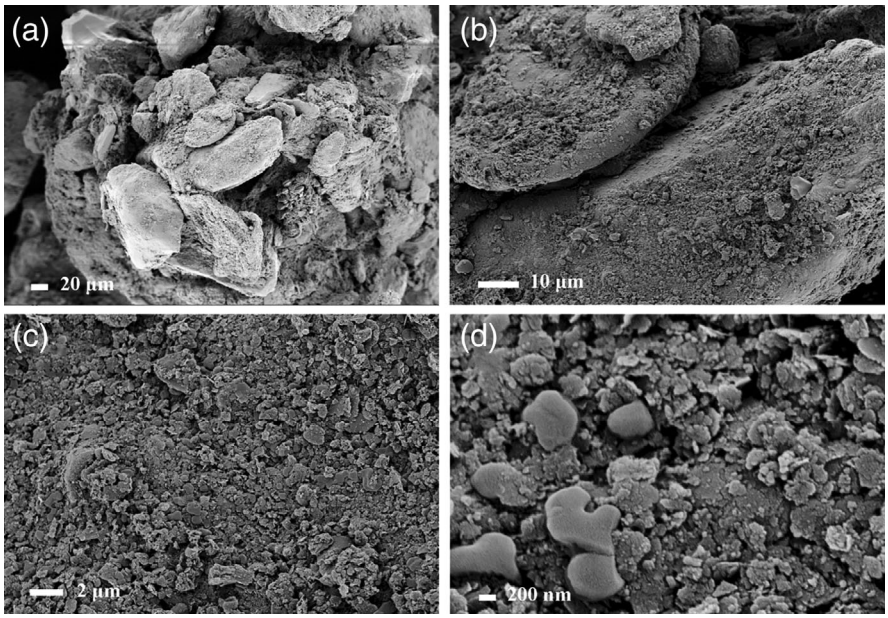

FIGURE 5 Low- and high-scanning electron microscopy images of leaf-based artificial soil

with soil minerals (e.g., the many clay minerals contain cations including Ca and Mg at their surface), thus keeping the nature of near pH neutrality as an important property of soil.

The corresponding EDX results (Figures S6 and S7) confirm that the carbon in AS is mainly bound to the mineral surface. We determine 30.5 wt % for wood-based artificial soil (W-AS) and 27.6 wt % for leaf-based artificial soil (L-AS), much higher than in the parental SS (6.7 wt %) and even higher than in cultivated soils (17.8 wt %). These values are higher than the corresponding values determined by chemical combustion analysis (discussed next), reflecting that EDX is a near-surface sensitive technique and that the carbon is indeed localized at the surface of the mineral particles but not within. The conjugation of A-SOM with the minerals is thereby quantified, thus complementing the qualitative visualization from the photographs (Figure S8). The content of the common elements of soil (O, Si, Fe, Al, K, Ca, and Mg) remains nearly constant (only relatively low due to the increased carbon content) before and after hydrothermal treatment. This underlines our assumption that the minerals are possibly surface etched for better coating but not changed in their structure and composition.

The data of EA to quantify the carbon content are displayed in Table 1. The carbon contents at the surface and in the bulk are expectedly very different, but the trend is the same, that is, AS shows a highly increased organic carbon content (0.55% in G-AS, 3.44% in W-AS, and 3.89% in L-AS) as compared with the SS precursor

Samples	Sandy soil	Cultivated soil	G-AS	W-AS	L-AS	Black soil
EDX (C %)	6.7	17.8	14.4	30.5	27.6	20.1
EA (C %)	0.02	2.92	0.55	3.44	3.89	10.3
SOM (%)	1.2	7.8	2.9	16.6	12.0	29.3

TABLE 1 Comparative carbon contents from elemental analysis and energy dispersive X-ray analysis and soil organic matter

Abbreviations: EA, elemental analysis; EDX, energy dispersive X-ray; G-AS, glucose-based AS; SOM, soil organic matter.

(0.02%). The enrichment at the surface is in all experiments of the order of a factor of 100. Figure S9 presents the relationships of carbon contents obtained from EA and EDX analyses with a classical SOM determination, indicating that EA results indeed agree with the SOM determination.

To our deep satisfaction, the synthesis of artificial SOM via HTH indeed increased SOM content in a depleted mineral soil, without having the ability to wash it away. The numbers are 1.2%, 7.8%, 2.9%, 16.6%, and 12.0% for SS, cultivated soil, G-AS, W-AS, and L-AS, respectively. We have chosen the biomass content in the primary synthesis in a way that the SOM is even larger than in the cultivated soil sample to allow subsequent dilution. Worth noting, this general approach gives us a promising method to prepare retrosynthesized BSs with a variety of compositions just through regulating the ratio of soils and biomass as well as the biomass type, and currently, samples were created with an amount of humic components, which exceeds natural BSs. Interestingly, AS can improve soil very well and not only increase SOM but also change soil structure, making them close to BSs, as concluded in Table S1. Another point that needs to be emphasized is that the as-prepared AS is fabricated under medium–high temperatures and pressure, that is, the product is sterile and free of microorganisms but also prions, peptides, DNA, or more complex organic molecules such as agricultural chemicals are decomposed and converted.

A use in plant breeding is favorably based on a mixture with real soils to establish an again active microbiome, that is, an also biologically fertile soil system. SEM images of simulated soils (mixtures of AS and SS), cultivated soil (Brandenburg, Germany black soil, GBS, Germany), and BS (Northeast China; Figures S10–S12) depict indeed similar rough surfaces so that mixing should occur without size depletion or differences in wettability.

An initial approximation to determine potential mineralogical variations was done with X-ray diffraction (XRD) on dried soil powders. As seen from Figure 6, nine peaks can be attributed to SiO_2 (Joint Committee on Powder Diffraction Standards no.78-2315) in the natural sand refill (the main component), centered at 20.7°, 26.6°, 36.5°, 39.5°, 40.3°, 42.4°, 45.8°, 50.1°, 54.9°, and 57.3°, respectively. In the cultivated soil from a neighboring Brandenburg source, BS from China and the other samples of activated and conjugated SS, the peaks assigned to the SiO_2 component decreased in intensities (highlighted in blue and green colors). Some other peaks representing other mineral components could also be assigned, such as $CaCO_3$, $Ca_2(SiO_4)$, CaMg (Si_2O_6), $MgSiO_3$, $Mg_2(Si_2O_6)$, Mg_2SiO_4, $Mg(SiO_3)$, and $Mg(SiO_3)$. Besides, the XRD profiles of five studied soils have some additional

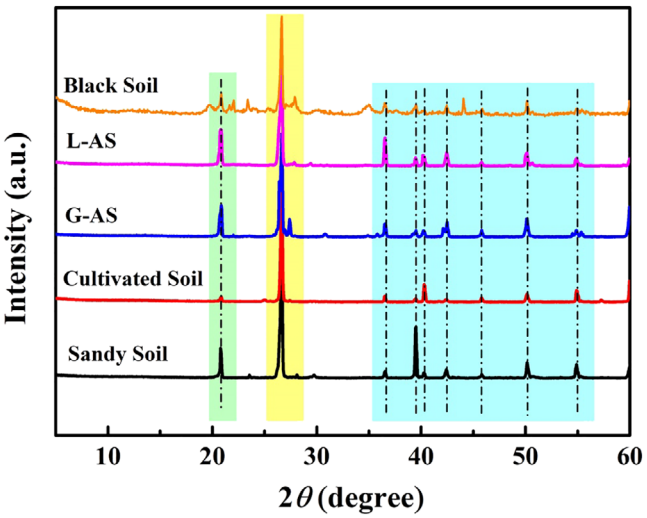

FIGURE 6 Comparative X-ray diffraction patterns of the as-prepared artificial soils and real soils [Colour figure can be viewed at wileyonlinelibrary.com]

small peaks located at 27.3°/27.8°, which may be attributed to iron or calcium phosphates or iron, calcium, and magnesium silicates.

The FTIR curves exhibit some differences among five studied soils (Figure 7a), with three strong peaks centered at 3,627, 1,637 and 1,537 cm^{-1}, respectively, for BS caused by stretching vibration of —OH, C═C, and C—N groups, different to the same regions on the other samples: two weak absorption peaks (3,357 and 1,640–1,620 cm^{-1}) are observed in the spectra of cultivated and AS. For all the curves, the existence of bands located at 1,100–1,000, 782, 692, and 600 cm^{-1} is attributed to the vibrations of C—O, C—H, —OH, and/or $—NH_2$ groups. Generally, FTIR curves in the range of 1,000–2,000 cm^{-1} allow for a better understanding of the chemical structure of SOM. Figure 7b–f shows more details in this region with the second derivative curves (inserts). This is a well-known tool to effectively separate the broadband absorption peaks of complex dense matter with the otherwise nearly invisible changes through added peaks. As expected, five main peaks at 1,717, 1,650, 1,616, 1,540, and 1,508 cm^{-1}, respectively, are identified in every curve, corresponding to vibration of C═O (—COOH), C═O (amides I), asymmetric COO—, C—N (amides II), and C═C (aromatics).

In order to examine the changes in different functional groups of the studied soils, peak-fitting results in two representative regions with semiquantitatively analysis are also presented in Figure 8; the peak areas come from FTIR fitting quantified in Table S2. In range of 2,800–3000 cm^{-1} representing aliphatic

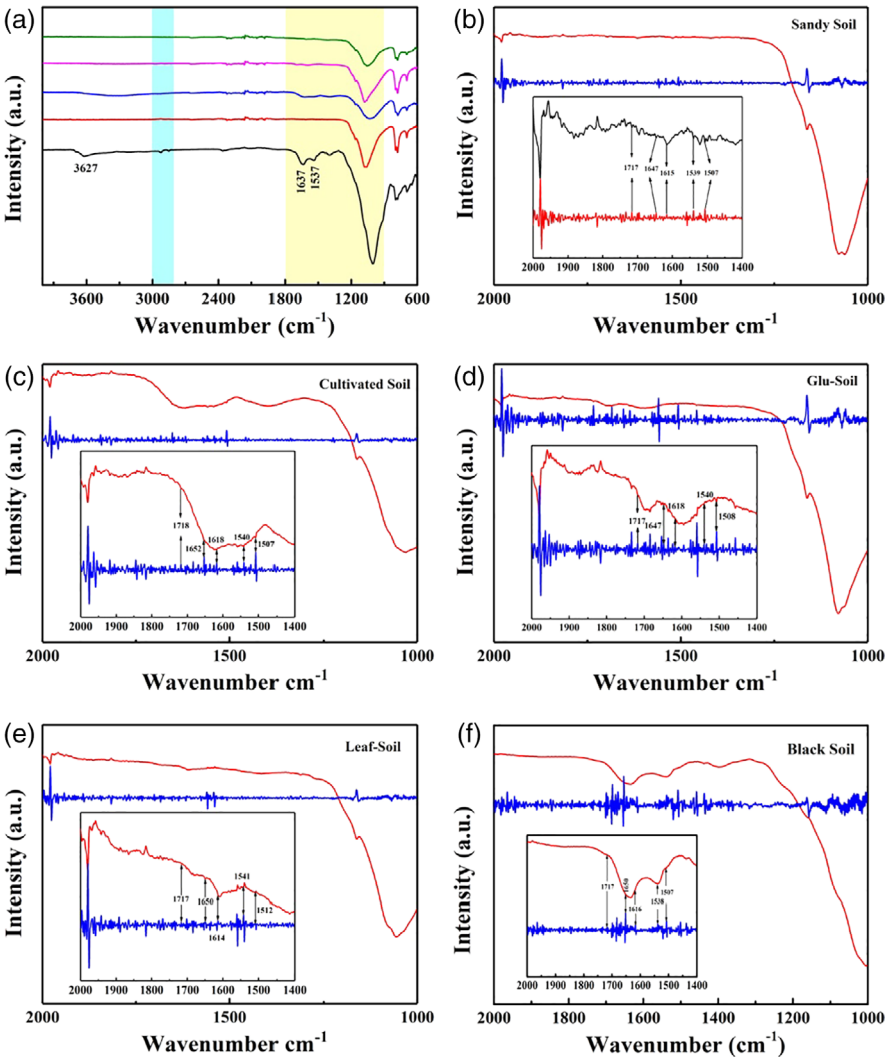

FIGURE 7 Fourier-transform infrared spectroscopy spectrum of the five studied soils (a) sandy soil, (b) cultivated soil, (c) glucose soil, (d) leaf soil, (e) and black soil (f), and the second derivative of the spectra at 1,000–2,000 cm^{-1} Fourier-transform infrared spectroscopy region [Colour figure can be viewed at wileyonlinelibrary.com]

structure with three characteristic peaks at around 2,960, 2,930 and 2,856 cm^{-1}, furthermore, relative peak areas in two bands at ~2,930 and ~2,960 cm^{-1} attributed to asymmetric —CH_2 and —CH_3 allow to estimate the length of aliphatic chains and degree of branching in side chains, that is, the area ratios in five studied soils are changing from 1.4–4.5, meaning that SS (2.52) has less but longer aliphatic chains and a lower degree of structural saturation, whereas synthesized samples can effectively moderate SS to match the spectra of fertile soil (1.5 for AS, 1.5 for GBS, and 1.4 for BS). Besides, another FTIR region of 800–1,800 cm^{-1} assigned to O-containing and aromatic structures can be divided into three peak groups in 1,650–1,800, 1,500–1,650 cm^{-1}, and 1,040–1,260 cm^{-1}. The *C* index (Equation (1); *A* = area) describes the area ratios representing peak groups in 1,650–1,800 and 1,500–1,650 cm^{-1}, thus results are 0.35, 0.21, 0.22, and 0.13 for sandy, cultivated, artificial, and BS, respectively, indicating an increase in humification level (Chen, Mastalerz, & Schimmelmann, 2012; Li & Zhu, 2014).

$$C\,\text{index} = \frac{A_{1,650-1,800}}{A_{1,650-1,800} + A_{1,500-1,650}}. \quad (1)$$

In addition, the area ratios of $A_{1,650-1,800}$ to $A_{1,500-1,650}$ and $A_{1,040-1,260}$ to $A_{1,500-1,650}$ follow an order of SS (0.54) > AS (0.28) > GBS (0.26) > BS (0.10) and SS (7.21) > AS (3.67) > GBS (2.57) > BS (2.02), indicating the increase of C-containing functional groups and a relative decrease of O-containing ones, in good agreement with EA results (Table S3). The BS is out of this comparison due to the different soil origin. Worth noting, artificial fulvic and humic acids obtained from glucose and crude biomass respectively exhibit rather big differences, including in the values of the *C* index (0.36 vs. 0.22), the ratios of $A_{1,650-1,800}$ to $A_{1,500-1,650}$ (0.55 vs. 0.28) and $A_{1,040-1,260}$ to $A_{1,500-1,650}$ (5.15 vs. 3.67); the as-formed AS by addition of lignin containing crude biomass is indeed closer to the data of real soil, reflecting the increase and match of humic substances. Therefore, we have chosen L-AS as a reference for AS for the following systematic soil property studies.

As discussed above, water and nutrition retention are two important evaluation criteria for determining soil fertility. Therefore, water retention and nutrient conservation are briefly tested in order to preliminarily evaluate the AS performance in comparison with real BS. Figure S13 depicts the experimental equipment for water and nutrient binding examinations with an initial 200-ml solution

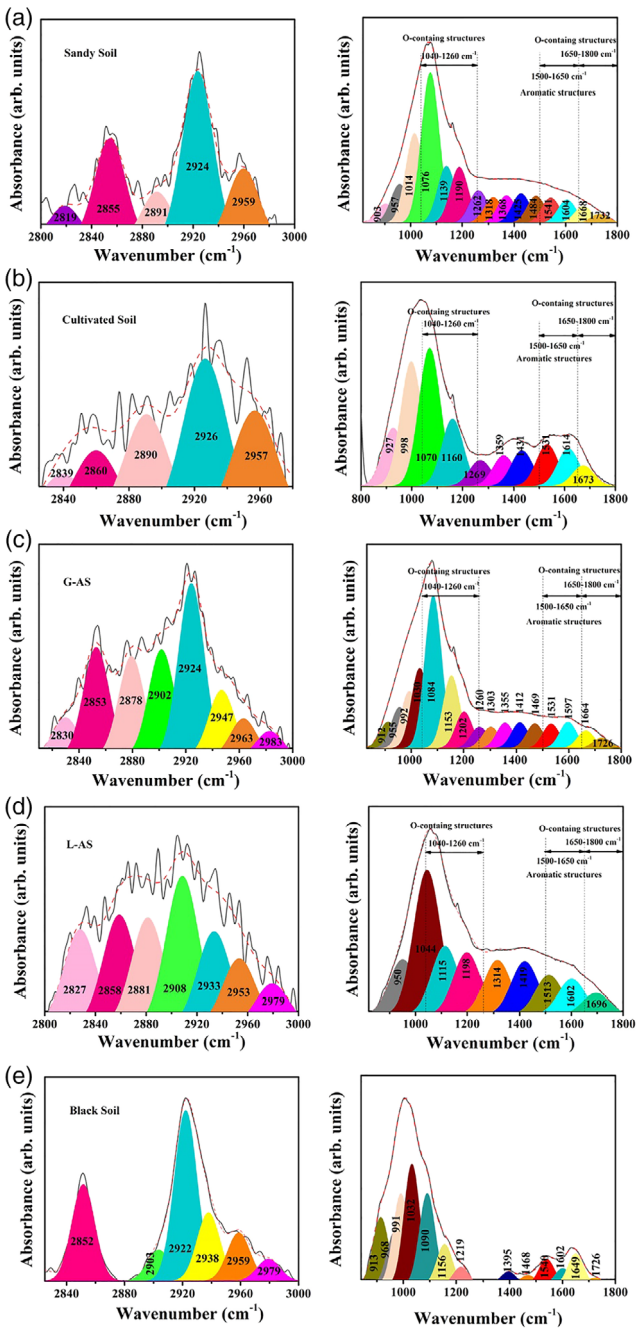

FIGURE 8 Curve-fitting Fourier-transform infrared spectroscopy spectra for five studied soils at 2,800–3,000 and 800–1,800 cm^{-1} Fourier-transform infrared spectroscopy region [Colour figure can be viewed at wileyonlinelibrary.com]

containing 1.0 mol L^{-1} KCl, NH_4Cl, and NaH_2PO_4 (these amounts clearly being beyond all possible absorption capacities, i.e., the soils are 'saturated') filtered through a column filled with 40 g of dry soil matter. Results of water and ion bonding in different soils are compared in Table 2, where the 'big three' nutrient elements (N, P, and K) are evaluated. Obviously, the pure AS (L-AS sample) has the strongest water retention (12.5%), opposite to the poorest retaining capacity of SS (7.5%) where L-AS is synthesized from. Interestingly, the mixture of SS and AS has a similar performance as cultivated soils (Germany)

TABLE 2 Comparative properties of water and ion bonding in different soils

Samples	Nutrient recovery			RLV (ml)
	N %	P %	K %	
sandy soil	2.6	19.6	1.8	185
Artificial soil	19.7	25.8	15.8	175
Mixtures[a]	12.8	23.6	14.0	183
Cultivated soil	11.3	15.7	6.9	183
Black soil	23.6	88.7	4.7	184

Abbreviation: RLV, remaining liquid volume.
[a]The mixture of sandy soil and artificial soil with the mass ratio of 1:1.

to hold water (8.5%). For the three typical fertilizer elements (N, P, and K), we found rather big differences between the various samples (SS, AS, mixture with same quantity of SS and AS, cultivated soils, and BS). The addition of AS greatly enhanced the ability of ion bonding in SS (12.8% vs. 2.6% in N element, 23.6% vs. 19.6% in P element, and 14.0% vs. 1.8% in K element), which can of course be related on the increase of SOM from 1.2% (SS) to 3.3% (after mixing with AS) but must contain an influence of activation of the mineral surface. These values are even higher than the values from cultivated soils (11.3% in N element, 15.7% in P element, and 6.9% in K element), thus preliminarily verifying the possibility of reproducing the ion binding of BS. In generalsss, the soils with high carbon content (reflecting SOM; Yao et al., 2017) present excellent performance, and the results of water and nutrient binding show a very good correlation.

4 | CONCLUSIONS

The application of the HTH process in the presence of a major mineral phase taken from real soil samples was analyzed. Humification in the presence of minerals increases the —OH functionality of the mineral surface to make it more hydrophilic, and the subsequent formation of organic acids promotes the intimate binding of organic materials to the mineral surface. Moreover, the content of common elements (O, Si, Fe, Al, K, Ca, and Mg) in the soil remains almost constant before and after hydrothermal treatment, indicating that the mineral surface etched to obtain a better coating. The SOM content in the synthetic AS is increased compared with the barren mineral soil, and the retrosynthesized BSs with various components are prepared by adjusting the ratio of soil and biomass and the type of biomass. The enhancement of SOMs can effectively improve the water and ion bonding of soil. Indeed, it was shown by water uptake and fertilizer saturation experiments that artificial humification greatly improves the ability of a soil to absorb K, N, and P components, together with an increased water binding capacity. These physicochemical experiments now set the base to agricultural experiments on the larger scale.

In general, the formation of natural humic substances in geological soil needs quite a long time, up to a few thousand years; it is based both on chemical as well as on biological processes, and the yield is

comparably low (Visser, 1962). This report aims to accelerate the underlying carbon fixation processes simply by chemical engineering means while keeping the carbon fixation yield close to complete. At the same time, both process and chemicals must be tuned that the artificial product is matching as much as possible with the composition and structure of real soils to find a suitable and sustainable approach for soil modification. Ideally this will access the process of 'terraforming' of weak or used-up soil matter to give fertile plating media.

ACKNOWLEDGMENTS

All authors appreciate the funding of the project by Max Planck Society. Dr. Yang acknowledges the financial supports from the National Natural Science Fund for Young Scholars (31600413), University Nursing Program for Young Scholars with Creative Talents in Heilongjiang Province (UNPYSCT-2017018), and Natural Science Foundation of Heilongjiang Province of China (QC2018019).

AUTHOR CONTRIBUTIONS

The manuscript was written through contributions of all authors. All authors have given approval to the final version of the manuscript. These authors contributed equally.

ORCID

Markus Antonietti https://orcid.org/0000-0002-8395-7558

REFERENCES

Bünemann, E. K., Bongiorno, G., Bai, Z., Creamer, R. E., De Deyn, G., de Goede, R., . . . Brussaard, L. (2018). Soil quality–A critical review. *Soil Biology and Biochemistry*, *120*, 105-125. https://doi.org/10.1016/j.soilbio.2018.01.030

Chabbi, A., Kögel-Knabner, I., & Rumpel, C. (2009). Stabilised carbon in subsoil horizons is located in spatially distinct parts of the soil profile. *Soil Biology and Biochemistry*, *41*(2), 256–261. https://doi.org/10.1016/j.soilbio.2008.10.033

Chen, Y., Mastalerz, M., & Schimmelmann, A. (2012). Characterization of chemical functional groups in macerals across different coal ranks via micro-FTIR spectroscopy. *International Journal of Coal Geology*, *104*, 22–33. https://doi.org/10.1016/j.envsci.2010.07.004

Cohen, J., Pfeiffer, K., & Francis, J. A. (2018). Warm Arctic episodes linked with increased frequency of extreme winter weather in the United States. *Nature Communications*, *9*(1), 869. https://doi.org/10.1038/s41467-018-02992-9

Cui, Y., Fang, L., Guo, X., Wang, X., Zhang, Y., Li, P., & Zhang, X. (2018). Ecoenzymatic stoichiometry and microbial nutrient limitation in rhizosphere soil in the arid area of the northern Loess Plateau, China. *Soil Biology and Biochemistry*, *116*, 11–21. https://doi.org/10.1016/j.soilbio.2017.09.025

Franko, U., & Merbach, I. (2017). Modelling soil organic matter dynamics on a bare fallow Chernozem soil in Central Germany. *Geoderma*, *303*, 93–98. https://doi.org/10.1016/j.geoderma.2017.05.013

Grüneberg, E., Schöning, I., Hessenmöller, D., Schulze, E. D., & Weisser, W. W. (2013). Organic layer and clay content control soil organic carbon stocks in density fractions of differently managed German beech forests. *Forest Ecology and Management*, *303*, 1–10. https://doi.org/10.1016/j.foreco.2013.03.014

Haberhauer, G., Rafferty, B., Strebl, F., & Gerzabek, M. (1998). Comparison of the composition of forest soil litter derived from three different sites at various decompositional stages using FTIR spectroscopy. *Geoderma*, *83*(3-4), 331–342. https://doi.org/10.1016/S0016-7061(98)00008-1

Hu, B., Wang, K., Wu, L., Yu, S. H., Antonietti, M., & Titirici, M. M. (2010). Engineering carbon materials from the hydrothermal carbonization process of biomass. *Advanced Materials*, *22*(7), 813-828. doi: https://doi.org/10.1002/adma.200902812

Jin, J., Sun, K., Wang, Z., Han, L., Wu, F., & Xing, B. (2016). The effect of composition on stability (14C activity) of soil organic matter fractions from the albic and black soils. *Science of The Total Environment*, *541*, 92–100. https://doi.org/10.1016/j.scitotenv.2015.09.041

Lal, R., Negassa, W., & Lorenz, K. (2015). Carbon sequestration in soil. *Current Opinion in Environmental Sustainability*, *15*, 79–86. https://doi.org/10.1016/j.cosust.2015.09.002

Lehmann, J., & Kleber, M. (2015). The contentious nature of soil organic matter. *Nature*, *528*, 60–68. https://doi.org/10.1038/nature16069

Li, W., & Zhu, Y. (2014). Structural characteristics of coal vitrinite during pyrolysis. *Energy & Fuels*, *28*(6), 3645–3654. https://doi.org/10.1021/ef500300r

Liu, X., Bai, X., Dong, L., Liang, J., Jin, Y., Wei, Y., … Qu, J. (2018). Composting enhances the removal of lead ions in aqueous solution by spent mushroom substrate: Biosorption and precipitation. *Journal of Cleaner Production*, *200*, 1–11. https://doi.org/10.1016/j.jclepro.2018.07.182

Lützow, M. v., Kögel-Knabner, I., Ekschmitt, K., Matzner, E., Guggenberger, G., Marschner, B., & Flessa, H. (2006). Stabilization of organic matter in temperate soils: Mechanisms and their relevance under different soil conditions–A review. *European Journal of Soil Science*, *57*(4), 426–445. https://doi.org/10.1111/j.1365-2389.2006.00809.x

Marshall, C., & Page, H. (1927). The origin of humic matter. *Nature*, *119*(2993), 393. https://doi.org/10.1038/119393a0

Nikiforoff, C. C. (1959). Reappraisal of the soil. *Pedogenesis consists of transactions in matter and energy between the soil and its surroundings*, *129*(3343), 186–196. https://doi.org/10.1126/science.129.3343.186

Patzel, N., Sticher, H., & Karlen, D. L. (2000). Soil fertility—Phenomenon and concept. *Journal of Plant Nutrition and Soil Science*, *163*(2), 129-142. doi:https://doi.org/10.1002/(SICI)1522-2624(200004)163:2<129::AID-JPLN129 > 3.0.CO;2-D

Schmidt, M. W., Torn, M. S., Abiven, S., Dittmar, T., Guggenberger, G., Janssens, I. A., … Manning, D. A. (2011). Persistence of soil organic matter as an ecosystem property. *Nature*, *478*(7367), 49–56. https://doi.org/10.1038/nature10386

Shepherd, T. G. (2016). Effects of a warming Arctic. *Science*, *353*(6303), 989–990. https://doi.org/10.1126/science.aag2349

Thiele-Bruhn, S., Leinweber, P., Eckhardt, K. U., Siem, H. K., & Blume, H. P. (2014). Chernozem properties of black soils in the Baltic region of Germany as revealed by mass-spectrometric fingerprinting of organic matter. *Geoderma*, *213*, 144–154. https://doi.org/10.1016/j.geoderma.2013.07.036

Titirici, M.-M., Thomas, A., & Antonietti, M. (2007). Back in the black: Hydrothermal carbonization of plant material as an efficient chemical process to treat the CO2 problem? *New Journal of Chemistry*, *31*(6), 787–789. https://doi.org/10.1039/B616045J

Varadachari, C., Mondal, A. H., Dulal, C., & N., & Ghosh, K. (1994). Clay-humus complexation: Effect of pH and the nature of bonding. *Soil Biology and Biochemistry*, *26*(9), 1145–1149. https://doi.org/10.1016/0038-0717(94)90136-8

Visser, S. A. (1962). Production of humic substances in decomposing peat and compost samples. *Nature*, *196*, 1211. doi::https://doi.org/10.1038/1961211b0

Xu, X. Z., Xu, Y., Chen, S. C., Xu, S. G., & Zhang, H. W. (2010). Soil loss and conservation in the black soil region of Northeast China: A retrospective study. *Environmental Science & Policy*, *13*(8), 793–800. https://doi.org/10.1016/j.envsci.2010.07.004

Yang, F., Zhang, S., Cheng, K., & Antonietti, M. (2019). A hydrothermal process to turn waste biomass into artificial fulvic and humic acids for soil remediation. *Science of The Total Environment*.. https://doi.org/10.1016/j.scitotenv.2019.06.045

Yang, X., Chen, X., & Yang, X. (2019). Effect of organic matter on phosphorus adsorption and desorption in a black soil from Northeast China. *Soil and Tillage Research*, *187*, 85–91. https://doi.org/10.1016/j.still.2018.11.016

Yao, Q., Liu, J., Yu, Z., Li, Y., Jin, J., Liu, X., & Wang, G. (2017). Three years of biochar amendment alters soil physiochemical properties and fungal community composition in a black soil of northeast China. *Soil Biology and Biochemistry*, *110*, 56–67. https://doi.org/10.1016/j.soilbio.2017.03.005

SUPPORTING INFORMATION

Additional supporting information may be found online in the Supporting Information section at the end of this article.

How to cite this article: Yang F, Zhang S, Fu Q, Antonietti M. Conjugation of artificial humic acids with inorganic soil matter to restore land for improved conservation of water and nutrients. *Land Degrad Dev*. 2020;31:884–893. https://doi.org/10.1002/ldr.3486